

Hydrogen Bonded OH-Stretching Vibration in the Water Dimer

Daniel P. Schofield,[†] Joseph R. Lane, and Henrik G. Kjaergaard*

Department of Chemistry, University of Otago, P.O. Box 56, Dunedin, New Zealand

Received: June 6, 2006; In Final Form: November 24, 2006

We have calculated the frequencies and intensities of the hydrogen-bonded OH-stretching transitions in the water dimer complex. The potential-energy curve and dipole-moment function are calculated ab initio at the coupled cluster with singles, doubles, and perturbative triples level of theory with correlation-consistent Dunning basis sets. The vibrational frequencies and wavefunctions are found from a numerical solution to a one-dimensional Schrödinger equation. The corresponding transition intensities are found from numerical integration of these vibrational wavefunctions with the ab initio calculated dipole moment function. We investigate the effect of counterpoise correcting both the potential-energy surface and dipole-moment function. We find that the effect of using a numeric potential is significant for higher overtones and that inclusion of a counterpoise correction for basis set superposition error is important.

Introduction

The hydrogen-bonded water dimer ($\text{H}_2\text{O}\cdot\text{H}_2\text{O}$) is the simplest water cluster. It serves as the first step between gas-phase and bulk-phase water and is likely to be an important atmospheric absorber of solar radiation.^{1–3} To accurately model solar absorption by the water dimer, knowledge of its absorption spectrum in the infrared and near-infrared regions is essential. However, at atmospherically relevant conditions, the gas-phase spectrum of the water dimer is inherently hard to record because of its relatively low equilibrium concentration compared with that of the water monomer and because of the overlap of $\text{H}_2\text{O}\cdot\text{H}_2\text{O}$ absorption features with those of water monomer (H_2O).^{1–7}

Perhaps the most interesting vibrational mode in $\text{H}_2\text{O}\cdot\text{H}_2\text{O}$ is the hydrogen-bonded OH_b -stretching motion. The frequency of this vibration is red-shifted significantly compared to the other OH-stretching vibrations of the water monomer and dimer.^{4,8} Previous calculations have shown that at high vibrational excitation, the OH_b -stretching transitions in $\text{H}_2\text{O}\cdot\text{H}_2\text{O}$ are shifted outside the spectral regions of strong monomer absorption.^{4,5}

The spectroscopy of the OH-stretching oscillator in $\text{H}_2\text{O}\cdot\text{H}_2\text{O}$ is complicated by an intensity pattern characteristic of hydrogen-bound OH_b -stretching modes.^{4,5,9–12} The intensity of the fundamental OH_b -stretching transition is much stronger and that of the first overtone is significantly weaker than the corresponding OH-stretching transitions in the monomer. The low intensity of the first overtone is attributable to a cancellation of terms in the dipole-moment expansion.^{10,11} As a result, most experiments in the first OH-stretching region have failed to identify the OH_b -stretching transition in $\text{H}_2\text{O}\cdot\text{H}_2\text{O}$.^{13–15} Recently, a very weak transition in a neon matrix experiment was assigned to the first OH-stretching overtone of $\text{H}_2\text{O}\cdot\text{H}_2\text{O}$.¹⁶

Experimental detection of higher OH_b -stretching overtone transitions in the water dimer has been limited to the band Pfeilsticker et al. observed in the atmosphere at 749.5 nm (13340 cm^{-1}), which displayed the expected quadratic dependence on

the water monomer pressure.¹⁷ This band was assigned to the third OH_b -stretching overtone transition in $\text{H}_2\text{O}\cdot\text{H}_2\text{O}$. Attempts to observe this third OH_b -stretching overtone transition in laboratory experiments have so far been unsuccessful.¹⁸ Suhm has suggested that this 19.4 cm^{-1} wide band is too narrow to be from the water dimer.^{19,20} Ptashnik et al. observed water dimer bands in the first stretch–bend combination region around 5500 cm^{-1} with widths of around $30\text{--}60\text{ cm}^{-1}$.^{1,3} These widths are comparable to the 70 cm^{-1} wide OH-stretch–COH-bend combination band recently measured in the trimethylamine–methanol complex.¹²

A comparison of measured and calculated transition intensities can provide equilibrium constants, which are very difficult to calculate accurately.^{21–25} Clearly, accurate knowledge of the water dimer equilibrium constant is crucial for assessment of its atmospheric importance. To aid the experimental efforts, accurate calculations of frequencies, intensities, and widths of these water dimer transitions are important.

In this work, we calculate the vibrational frequencies and intensities of the OH-stretching transitions in $\text{H}_2\text{O}\cdot\text{H}_2\text{O}$. We investigate several factors that influence the calculated OH_b -stretching transitions to assess the accuracy of the previously calculated results and further aid experimental detection of the $\text{H}_2\text{O}\cdot\text{H}_2\text{O}$ overtone transitions. These factors include the suitability of the Morse function to describe higher overtones of this highly anharmonic OH_b -stretching mode, the effect of a limited basis set, and the impact of basis set superposition error. The calculated OH-stretching frequencies are also compared to the results obtained for water monomer.

Theory and Calculations

The dimensionless oscillator strength f of a transition from the vibrational ground state $|0\rangle$ to a vibrationally excited state $|v\rangle$ is given by²⁶

$$f_{v0} = 4.702 \times 10^{-7} [\text{cm D}^{-2}] \tilde{\nu}_{v0} |\bar{\mu}_{v0}|^2 \quad (1)$$

where $\tilde{\nu}_{v0}$ is the vibrational wavenumber of the transition in cm^{-1} and $\bar{\mu}_{v0} = \langle v|\bar{\mu}|0\rangle$ is the transition dipole matrix element in debye.

* To whom correspondence should be addressed. E-mail: henrik@alkali.otago.ac.nz. Fax: 64-3-479-7906. Phone: 64-3-479-5378.

[†] Present address: Department of Chemistry and Center for Molecular and Materials Simulations, University of Pittsburgh, Pittsburgh, PA 15260.

We use two approaches to calculate the energies and intensities of the one-dimensional (1D) OH_b-stretching anharmonic oscillator (AO) in the water dimer. The first approach assumes a Morse oscillator, with the vibrational energy levels given by

$$E(v)/(hc) = \left(v + \frac{1}{2}\right)\tilde{\omega} - \left(v + \frac{1}{2}\right)^2\tilde{\omega}x \quad (2)$$

The Morse oscillator frequency $\tilde{\omega}$ and anharmonicity $\tilde{\omega}x$ are found from the second-, third-, and fourth-order derivatives of the potential-energy curve as described previously.^{27–29} The derivatives are found by fitting an eighth-order polynomial to a nine-point ab initio calculated potential-energy curve, obtained by displacing the OH_b bond from -0.2 to 0.2 Å in 0.05 Å steps around equilibrium. This ensures converged derivatives.

In the second approach the 1D Schrödinger equation is solved numerically using a finite element method to give both the vibrational energy levels and wavefunctions.³⁰ The potential energy curve used for this covers the range from -0.3 to 0.6 Å in 0.025 Å steps around equilibrium. This ensures converged energy levels (better than 0.1 cm⁻¹) and wavefunctions (f better than 0.1% for $v \leq 5$).

The transition dipole matrix element of eq 1 can be expanded as

$$\langle v|\bar{\mu}|0\rangle = \frac{\partial\bar{\mu}}{\partial q}\langle v|q|0\rangle + \frac{1}{2}\frac{\partial^2\bar{\mu}}{\partial q^2}\langle v|q^2|0\rangle + \frac{1}{6}\frac{\partial^3\bar{\mu}}{\partial q^3}\langle v|q^3|0\rangle + \dots \quad (3)$$

where q is the internal vibrational displacement coordinate. The integrals $\langle v|q^n|0\rangle$ required for the transition dipole moment are evaluated analytically for the Morse potential³¹ and by trapezoidal numeric integration for the numerical potential. The dipole moment coefficients are found from a sixth-order polynomial fit to a nine-point dipole moment curve calculated over values of q from -0.2 to 0.2 Å in 0.05 Å steps. The expansion in eq 3 is limited to sixth order.

We have used the harmonically coupled anharmonic oscillator (HCAO) local-mode model to estimate the effect of vibrational mode coupling on the OH_b-stretching transitions.³² We perform the three-dimensional (3D) HCAO vibrational calculation only for the hydrogen-donor unit (H_bOH_f) of the water dimer. The expression for the 3D Hamiltonian and dipole moment function that we use are similar to those used previously³³ and are given in the Supporting Information.

All ab initio calculations were performed at the coupled-cluster singles, doubles, and perturbative triples (CCSD(T)) level of theory with the Dunning-type correlation-consistent basis sets, aug-cc-pVXZ, where X = D, T, Q (AVXZ). In addition, we have used composite basis sets consisting of AVTZ, AVQZ, or AV5Z on the OH_b...O atoms and a reduced basis set, cc-pVTZ on the remaining hydrogens. We label these composite basis sets A'VTZ, A'VQZ, and A'V5Z. The 3D HCAO local mode calculation was only done with the CCSD(T)/AVTZ method.

The counterpoise (CP) correction scheme of Simon et al. was used to determine the CP-corrected potential-energy surface.³⁴ In a similar manner, we have determined the CP-corrected dipole moment as

$$\bar{\mu}_{AB}^{\text{CP}} = \bar{\mu}_{AB} + \bar{\mu}_A + \bar{\mu}_B - \bar{\mu}_A^* - \bar{\mu}_B^* \quad (4)$$

where $\bar{\mu}_{AB}$ represents the dipole moment of the complex, $\bar{\mu}_A$ and $\bar{\mu}_B$ are the dipole moments of the individual monomers at their complex geometry, and $\bar{\mu}_A^*$ and $\bar{\mu}_B^*$ are the dipole mo-

TABLE 1: Calculated OH_b-Stretching Frequencies (in cm⁻¹) and Intensities in the Water Dimer^a

Δv	AO (1D)		HCAO (3D)	
	$\tilde{\nu}$	f	$\tilde{\nu}$	f
1	3573.3	6.9×10^{-5}	3564.6	5.7×10^{-5}
2	6967.9	7.4×10^{-9}	6978.5	1.1×10^{-8}
3	10 183.7	8.3×10^{-10}	10 159.8	5.2×10^{-10}
4	13 220.7	2.8×10^{-10}	13 190.1	2.2×10^{-10}
5	16 079.0	4.6×10^{-11}	16 052.0	4.1×10^{-11}

^a Local-mode parameters and dipole-moment function obtained with the CCSD(T)/AVTZ ab initio method for both calculations.

ments of the individual monomers at their complex geometry calculated with “ghost” orbitals.

Harmonic normal-mode frequencies were calculated with the CCSD(T)/AVTZ method and are given in the Supporting Information. All coupled-cluster calculations assume a frozen core (O:1s). The dipole moment at each geometry is calculated using a finite field approach with a field strength of ± 0.005 a.u. All calculations were performed with MOLPRO 2002.6.³⁵

Results and Discussion

In Table 1 we compare the OH_b-stretching frequencies obtained from a 1D anharmonic oscillator (AO) calculation to those found from a 3D HCAO calculation. In both models, the AOs are described as Morse oscillators. The difference between the frequencies and intensities in Table 1 is entirely the result of the effect of vibrational coupling and mixed dipole-moment derivatives. The effect of vibrational coupling on the OH_b-stretching frequencies is reasonably small, as expected from the significantly different harmonic frequencies of the OH_b- and OH_f-stretching modes. The transition intensities are reduced upon inclusion of vibrational coupling for all but the first overtone. However, this transition is inherently weak because of cancellations of terms, and hence, it is more sensitive to coupling.¹¹ The change in intensity is less than 50% for all transitions investigated. The fact that the intensities decrease is consistent with the intense OH_b-stretching state sharing intensity with inherently weaker transitions to combination states. These changes in frequencies and intensities at the CCSD(T)/AVTZ level are likely transparent to higher-level methods, where it is not feasible to do the 3D calculations.

Previously, the harmonically coupled anharmonic oscillator local mode (HCAO) model has been used to calculate fundamental and overtone vibrational frequencies and intensities of the OH-stretching and HOH-bending transitions in the water dimer.^{4,5} The results of these calculations are in good agreement with observed fundamental and first overtone transitions.^{3,13–16} Calculations that include all 12 vibrational modes in H₂O•H₂O have used correlation-consistent vibrational self-consistent field,³⁶ harmonic normal mode,³⁷ or vibrational perturbation methods built into Gaussian 03.^{16,38} These calculations mainly yield fundamental and first overtone frequencies and are necessarily at a limited ab initio level. For the OH-stretching and HOH-bending transitions, the results obtained with the 12D methods do not seem better than those obtained with the HCAO local mode model.⁵

Morse versus Numeric Potentials. The CCSD(T)/AVTZ calculated potential energy curve and the corresponding energy levels are shown in Figure 1. The calculation of perturbative triples is known to fail at large bond displacements from equilibrium,³⁹ whereas the coupled cluster with singles and doubles method (CCSD) does not have this problem. We have

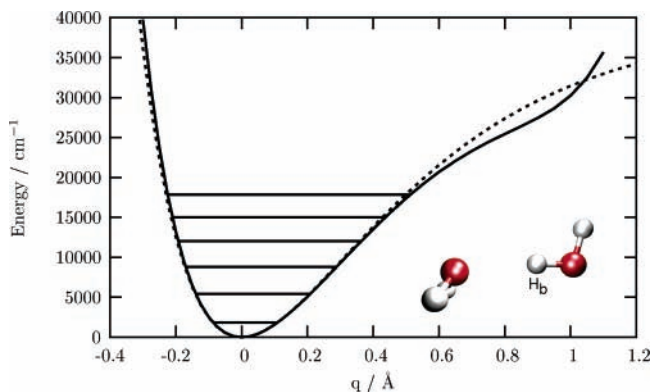


Figure 1. CCSD(T)/AVTZ-calculated OH_b -stretching potential-energy curve in the water dimer. The first six energy levels are shown. The dashed line represents the Morse potential obtained at the same level of theory.

TABLE 2: Calculated OH_b -Stretching Frequencies (in cm^{-1}) and Intensities^a

$\Delta\nu$	Morse		numeric	
	$\tilde{\nu}$	f	$\tilde{\nu}$	f
1	3584.6	6.9×10^{-5}	3584.6	6.9×10^{-5}
2	6984.8	9.6×10^{-9}	6983.1	1.8×10^{-8}
3	10 200.5	1.4×10^{-9}	10 192.6	2.4×10^{-9}
4	13 231.7	3.8×10^{-10}	13 207.8	6.7×10^{-10}
5	16 078.5	5.8×10^{-11}	16 020.9	1.1×10^{-10}

^a Calculated with the CCSD(T)/AVQZ dipole-moment function and potentials.

also calculated the CCSD/AVTZ potential-energy curve, which is similar to the CCSD(T)/AVTZ curve in the range shown in Figure 1.

At large positive displacements from equilibrium, the H_b atom comes into close proximity to the oxygen atom of the acceptor unit. This causes the OH_b -stretching potential to have a different shape from that of a normal diatomic molecule. As shown in Figure 1, both walls of the OH_b -stretching potential are repulsive. At $q \approx 0.9 \text{ \AA}$, there is a depression in the repulsive wall, which is consistent with an unstable $\text{H}_3\text{O}^+\cdot\text{OH}^-$ diionic structure. The lowest 6 energy levels lie within the potential calculated in the displacement range used in our numerical calculation. The Morse potential obtained from CCSD(T)/AVTZ calculated points in the $\pm 0.2 \text{ \AA}$ range is also shown in Figure 1. The Morse and numeric potentials are quite similar in the range covered by the first six energy levels. Not surprisingly, the discrepancy increases with increasing energy.

The CCSD(T)/AVQZ OH_b -stretching frequencies and intensities calculated for the Morse and numerical potentials are given in Table 2. For the fundamental transition the frequency and intensity calculated with the two methods is virtually the same. The frequencies calculated with the two methods diverge for increasing $\Delta\nu$, up to 60 cm^{-1} at $\Delta\nu = 5$. With the smaller AVTZ basis set, the difference increases to 100 cm^{-1} at $\Delta\nu = 5$.

This suggests, as expected, that the Morse potential is an adequate approximation in the lower-energy region of the potential, but it becomes less suitable to describe the highly vibrationally excited region.

The overtone intensities obtained for the numeric potential are about a factor of 1.8 larger than the Morse calculated intensities. The large difference in calculated intensity is caused by the difference in the wavefunctions since the same dipole moment function is used with both methods. Similar to the frequencies, we would have expected the discrepancy between the two methods to increase with $\Delta\nu$. The larger than expected

TABLE 3: Calculated OH_b -Stretching Frequencies (in cm^{-1}) with Numeric Potentials^a

$\Delta\nu$	A'VTZ	AVTZ	A'VQZ	AVQZ	A'V5Z	exptl ^b
1	3573.3	3571.9	3584.2	3584.6	3589.2	3601
2	6963.5	6960.6	6982.0	6983.1	6992.3	7018
3	10 166.2	10 161.7	10 190.2	10 192.6	10 205.9	
4	13 175.2	13 169.1	13 203.6	13 207.8	13 224.7	13 340
5	15 981.8	15 974.1	16 014.1	16 020.9	16 040.3	
N_{basis}	157	184	248	344	376	

^a Calculated with the CCSD(T) theory. ^b Values are taken from refs 8, 16, and 17.

TABLE 4: Calculated OH_b -Stretching Intensities with Numeric Potentials^a

$\Delta\nu$	A'VTZ	AVTZ	A'VQZ	AVQZ
1	6.9×10^{-5}	6.9×10^{-5}	7.0×10^{-5}	6.9×10^{-5}
2	1.4×10^{-8}	1.4×10^{-8}	1.7×10^{-8}	1.8×10^{-8}
3	2.0×10^{-9}	2.0×10^{-9}	2.3×10^{-9}	2.4×10^{-9}
4	5.4×10^{-10}	5.7×10^{-10}	6.8×10^{-10}	6.7×10^{-10}
5	8.4×10^{-11}	9.7×10^{-11}	1.1×10^{-10}	1.1×10^{-10}

^a Calculated with the CCSD(T) theory.

discrepancy for $\Delta\nu = 2$ and 3 is likely caused by a cancellation of terms in the transition dipole-moment expansion (eq 3), which makes these transitions weak.¹¹ In that case, a small change in the $\langle\nu|q^n|0\rangle$ matrix elements can lead to a large change in the calculated intensity.

Basis Set Effects. In Table 3, we show the calculated OH_b -stretching frequencies for numeric potentials obtained with different basis sets. We have used the full AVTZ and AVQZ basis sets and the composite basis sets A'VTZ, A'VQZ, and A'V5Z.

The calculated transition frequencies with the composite basis sets A'VTZ and A'VQZ are in excellent agreement with the results of the full AVTZ and AVQZ calculations. This indicates that use of selectively augmented composite basis sets can provide frequencies at significantly lower computational cost and suggests that the results of the A'V5Z basis set are similar to those with the full AV5Z basis set.²⁸

The calculated fundamental transition frequencies increase and become in better agreement with the experimental frequencies as the basis set increases in size. This is consistent with previous studies on small diatomic molecules.⁴⁰ The difference between calculated and experimental values seems to increase with increasing vibrational quantum number, although the experimental data are still uncertain. The transition frequencies appear to be converging with increasing basis set size but are not fully converged. The frequencies at the largest basis set (A'V5Z) are lower than those observed experimentally. If it was computationally feasible, an increase in the level of ab initio theory would likely lower the frequencies somewhat.⁴¹ We believe that this reduction will be of comparable size to the increase in frequency obtained from increasing to the complete basis set limit.^{40,41}

In Table 4, we show the calculated OH_b -stretching intensities for different basis sets. The fundamental intensity shows little change with basis set, as expected. The variation in overtone intensities with basis set is less than 30%.

Basis Set Superposition Error. The effect of an increasingly larger basis set on a complex such as water dimer is not as straightforward as that for an isolated molecule. Basis set superposition error (BSSE) leads to an artificial increase in the binding energy of water dimer, which decreases the intermolecular distance and increases the OH_b bond length. The net result of this is an underestimation of the OH_b -stretching

TABLE 5: Calculated OH_b-Stretching Frequencies (in cm⁻¹) and Intensities^a

$\Delta\nu$	non-CP		CP	
	$\tilde{\nu}$	f	$\tilde{\nu}$	f
1	3571.9	6.9×10^{-5}	3581.1	6.4×10^{-5}
2	6960.6	1.4×10^{-8}	6981.6	1.9×10^{-8}
3	10 161.7	2.0×10^{-9}	10 198.1	2.8×10^{-9}
4	13 169.1	5.7×10^{-10}	13 225.4	6.5×10^{-10}
5	15 974.1	9.7×10^{-11}	16 056.5	1.0×10^{-10}

^a Calculated with the CCSD(T)/AVTZ numeric potential.

frequency. To investigate the effect that BSSE has on the calculated transition frequencies and intensities of water dimer, we have applied a counterpoise (CP) correction.³⁴ We have optimized the water dimer structure both with and without a CP correction scheme at the CCSD(T)/AVTZ level of theory. These two structures are given in the Supporting Information. The most significant difference is a 0.03 Å elongation of the O...O distance and a 0.0002 Å contraction of the OH bond length. The binding energy of water dimer with the standard optimization is 5.2 kcal mol⁻¹, and with the CP optimization, this is lowered to 4.2 kcal mol⁻¹.

The calculated OH_b-stretching transition frequencies and intensities obtained with the non-CP- and CP-corrected potential-energy curve and dipole-moment function are given in Table 5. The CP-corrected frequencies are higher than those calculated from the non-CP-corrected potential-energy curve as expected from the decreased OH bond length. The highest-energy transitions are the most affected, with a 75 cm⁻¹ increase in $\tilde{\nu}$ for the $\Delta\nu=5$ transition. The CP corrected intensities are similar to those calculated without the CP correction. The change in intensity is ~10% for the $\Delta\nu=1, 4,$ and 5 transitions and ~40% for the $\Delta\nu=2$ and 3 transitions. The larger discrepancy for $\Delta\nu=2$ and 3 is likely caused by the aforementioned cancellation effects. The CP-corrected AVTZ frequencies and intensities are similar to the non-CP-corrected AVQZ results given in Table 2. This suggests that AVQZ quality results for vibrational frequencies and intensities in molecular complexes can be obtained from the significantly less-demanding CP-corrected AVTZ calculations.

Summary

Experimental observations of the OH_b-stretching transitions for water dimer are limited and only the fundamental transition has been repeatedly observed.^{8,42,43} The $\Delta\nu=2$ transition is very weak and has only been assigned in a Ne matrix study and not in the previous Ar or N₂ matrix studies.^{14,15,44} The atmospherically observed $\Delta\nu=4$ transition has been questioned because of its narrow bandwidth and has not been confirmed by laboratory experiments.^{17–19} Thus, it is difficult to estimate the uncertainties in our calculation on the basis of comparison to experiment.

The 1D local mode description of the OH_b-stretching transitions in water dimer is somewhat crude, necessitated by the desire to assess the effect of high-level ab initio calculations. The additional coupling in a multidimensional model would alter the frequency of the calculated 1D transitions. The HCAO 3D calculations presented include harmonic and cubic coupling between the two OH-stretching modes and the bending mode and give us an estimate of the effect of coupling in the H₂OH_f unit. Previous calculations on the water monomer show that the effect of higher-order anharmonic couplings, and a full variational treatment changes the HCAO fundamental frequency by as much as 30 cm⁻¹.^{1,32}

TABLE 6: Shifts of the OH_b-Stretching Frequencies (in cm⁻¹) Compared to the OH-Stretching Frequency in Water Monomer^a

$\Delta\nu$	AVTZ	AVQZ	A'V5Z ^b
1	136	141	140
2	298	308	306
3	490	506	504
4	719	742	740
5	996	1025	1025

^a Calculated with CCSD(T) numeric potentials. ^b Water monomer CCSD(T)/AV5Z frequency minus water dimer CCSD(T)/A'V5Z frequency.

We estimate the frequency of OH_b-stretching transitions in two different ways. First, we correct our calculated absolute frequencies for the deficiencies in our model. Second, we compare the red shift in our calculated frequencies for the OH-stretching modes in the water monomer and dimer and estimate the OH_b-frequency by subtracting this red shift from the experimental values for the water monomer. Both of these approaches are based on different assumptions, and the difference in the estimated frequencies provides some insight into the uncertainty.

We have made a qualified estimate of the frequency of the fundamental OH_b-stretching transitions solely on the basis of the present water dimer calculations. The effect of vibrational coupling is to lower the frequency ~10 cm⁻¹, and the CP correction increases the frequency by ~10 cm⁻¹. Increasing the basis set from A'V5Z to the complete basis set limit would probably add around 5 cm⁻¹, and improving the level of theory beyond CCSD(T) is expected to lower the frequency by around 5 cm⁻¹.⁴¹ We see that all these estimated corrections approximately cancel and that the AV'5Z frequency of 3590 cm⁻¹ is a reasonable estimate for the fundamental frequency, in good agreement with the experimental value of 3601 cm⁻¹.⁸

We have compared our calculations for the OH_b-stretching mode in water dimer with 1D calculations for the OH-stretching local mode in the water monomer. The water monomer calculations have been performed in a similar manner to our water dimer calculations, with transition energies and intensities found from a numerical solution to an ab initio calculated 1D potential. This comparison is not completely satisfactory because of the different level of coupling in the water monomer and the H₂OH_f unit in the water dimer. The effective vibrational coupling between the two equivalent OH-stretching modes in water monomer is more significant than that between the two nonequivalent OH-stretching modes in the H₂OH_f unit in water dimer. Furthermore, BSSE, which has a noticeable impact on the water dimer results, has no effect on the water monomer calculations.

In Table 6, we compare the red shift of the calculated OH_b-stretching frequency from the calculated OH-stretching frequency of the water monomer. We find that these frequency red shifts rapidly converge with basis set size. We can use these calculated red shifts to estimate the OH_b-stretching frequency by comparing to the water monomer observed transitions.

Within the local mode picture, the calculated OH-stretching frequencies in water should be compared with the average of the observed symmetric and antisymmetric OH-stretching modes. In the fundamental region, this average is 3706 cm⁻¹.⁴⁵ If we subtract the A'V5Z calculated red shift and include a correction for BSSE, from Tables 6 and 5, respectively, the value obtained is 3575 cm⁻¹, within 15 cm⁻¹ of the value obtained from our absolute calculation. Clearly these corrections increase with ν and are more difficult to estimate for the higher overtones.

The most discussed overtone transition is without doubt the $\Delta\nu = 4$ transition. The average of the observed symmetric and antisymmetric $\Delta\nu = 4$ transitions in water is $\sim 13\,829\text{ cm}^{-1}$.⁴⁵ If we subtract the A'V5Z redshift from Table 6 and add the CP correction from Table 5, we obtain an estimated position of $13\,145\text{ cm}^{-1}$. In comparison, if we take the absolute A'V5Z frequency from Table 3, add the CP correction, and subtract the coupling from Tables 5 and 1, respectively, we get a transition frequency of $13\,251\text{ cm}^{-1}$. The corrections from increasing the basis and level of theory are likely to cancel. Additional coupling in the vibrational model will lower the $13\,251\text{ cm}^{-1}$ value further and bring it closer to the value estimated from the frequency shifts. These estimated frequencies for the $\Delta\nu = 4$ transition are $\sim 200\text{ cm}^{-1}$ to the red of the previous estimates.^{4,5}

We have also calculated the intensities for the OH-stretching transition in water monomer with the 1D model. The CCSD(T)/AV5Z numeric potential intensities agree well with the experimental intensities (sum of symmetric and asymmetric OH-stretching transitions) despite the lack of vibrational coupling. For $\Delta\nu = 1-3$, the discrepancy is $\sim 10\%$; for $\Delta\nu = 4$, it is $\sim 20\%$, and for $\Delta\nu = 5$, it is $\sim 30\%$. For the higher overtones, $\Delta\nu = 4$ and 5 , the use of the numerical potential is important. The OH_b-stretching intensities in water dimer can be estimated from the calculated intensities in Tables 1, 4, and 5. For the fundamental transition, the CP-corrected AVTZ oscillator strength is 6.4×10^{-5} , which is lowered to about $\sim 5 \times 10^{-5}$ by the vibrational coupling. Increasing the basis set beyond AVTZ has little effect on this value. Experimental absolute OH-stretching intensities for the water dimer are limited to the very recent helium droplet fundamental intensity of 2.5×10^{-5} .⁴³ For the $\Delta\nu = 4$ overtone, the effect of increasing the basis set and including coupling are about 20–30% and to some extent cancel, and we estimate an intensity of $\sim 6 \times 10^{-10}$. This estimated intensity is about a factor of 2 higher than the previously published results for the OH_b-stretching transitions.^{4,5}

Conclusions

We have calculated frequencies and intensities of the hydrogen-bonded OH-stretching vibration in water dimer. The potential-energy curve and dipole-moment function are obtained from high-level CCSD(T) calculations. The effect of using a numeric potential rather than the Morse potential is significant for higher overtones and inclusion of a counterpoise correction for basis set superposition error is important. We find that our calculated frequencies are slightly lower than those previously calculated and for the fundamental also slightly lower than the observed frequency. Our calculated intensities are higher than those previously calculated, which would decrease water dimer equilibrium constants derived from these transitions.

Acknowledgment. We are grateful to Jeppe Olsen for use of his ONEDIM program. We thank Anna Garden, Tim Robinson, and Poul Jørgensen for helpful discussions. J.R.L. is grateful to the Foundation for Research, Science and Technology for a Bright Futures scholarship and H.G.K. to the Research Foundation at Aarhus University for a visiting professorship. We acknowledge the Lasers and Applications Research Theme at the University of Otago for use of their computer facilities. We thank the University of Otago Research Committee for a University of Otago Postgraduate Publishing Award. We acknowledge the Marsden Fund and the International Science

and Technology (ISAT) Linkage Fund administered by the Royal Society of New Zealand for support.

Supporting Information Available: The expression for the Hamiltonian, dipole-moment function, and CCSD(T)/AVTZ local-mode parameters used in the 3D HCAO calculation; the CCSD(T)/AVTZ and CCSD(T)/AVQZ AO local-mode parameters; the non-CP- and CP-optimized CCSD(T)/AVTZ geometries in Z-matrix format; and harmonic normal-mode frequencies calculated with the CCSD(T)/AVTZ method. This material is available free of charge via the Internet at <http://pubs.acs.org>.

References and Notes

- (1) Vaida, V.; Daniel, J. S.; Kjaergaard, H. G.; Goss, L. M.; Tuck, A. F. *Q. J. R. Meteorol. Soc.* **2001**, *127*, 1627–1643.
- (2) Daniel, J. S.; Solomon, S.; Kjaergaard, H. G.; Schofield, D. P. *Geophys. Res. Lett.* **2004**, *31*, L06118.
- (3) Ptashnik, I. V.; Smith, K. M.; Shine, K. P.; Newnham, D. A. *Q. J. R. Meteorol. Soc.* **2004**, *130*, 2391–2408.
- (4) Low, G. R.; Kjaergaard, H. G. *J. Chem. Phys.* **1999**, *110*, 9104–9115.
- (5) Schofield, D. P.; Kjaergaard, H. G. *Phys. Chem. Chem. Phys.* **2003**, *5*, 3100–3105.
- (6) Daniel, J.; Solomon, S.; Saunders, R.; Portman, R.; Miller, D.; Medsen, W. *J. Geophys. Res.* **1999**, *104*, 16785–16791.
- (7) Hill, C.; Jones, R. *J. Geophys. Res.* **2000**, *105*, 9421–9428.
- (8) Huisken, F.; Kaloudis, M.; Kulcke, A. *J. Chem. Phys.* **1996**, *104*, 17–25.
- (9) Badger, R. M.; Bauer, S. H. *J. Chem. Phys.* **1937**, *5*, 369–370, 31
- (10) Di Paolo, T.; Bourdéron, C.; Sandorfy, C. *Can. J. Chem.* **1972**, *50*, 3161–3166.
- (11) Kjaergaard, H. G.; Low, G. R.; Robinson, T. W.; Howard, D. L. *J. Phys. Chem. A* **2002**, *106*, 8955–8962.
- (12) Howard, D. L.; Kjaergaard, H. G. *J. Phys. Chem. A* **2006**, *110*, 9597–9601.
- (13) Nizkorodov, S. A.; Ziemkiewicz, M.; Nesbitt, D. J.; Knight, A. E. W. *J. Chem. Phys.* **2005**, *122*, 194316.
- (14) Perchard, J. P. *Chem. Phys.* **2001**, *273*, 217–233.
- (15) Perchard, J. P. *Chem. Phys.* **2001**, *266*, 109–124.
- (16) Bouteiller, Y.; Perchard, J. P. *Chem. Phys.* **2004**, *305*, 1–12.
- (17) Pfeilsticker, K.; Lotter, A.; Peters, C.; Bösch, H. *Science* **2003**, *300*, 2078–2080.
- (18) Kassi, S.; Macko, P.; Naumenko, O.; Campargue, A. *Phys. Chem. Chem. Phys.* **2005**, *7*, 2460–2467.
- (19) Suhm, M. *Science* **2004**, *304*, 823.
- (20) Pfeilsticker, K. *Science* **2004**, *304*, 823–824.
- (21) Goldman, N.; Leforestier, C.; Saykally, R. J. *J. Phys. Chem. A* **2004**, *108*, 787–794.
- (22) Schenter, G. K.; Kathmann, S. M.; Garrett, B. C. *J. Phys. Chem. A* **2002**, *106*, 1557–1566.
- (23) Vaida, V.; Headrick, J. E. *J. Phys. Chem. A* **2000**, *104*, 5401–5412.
- (24) Evans, G.; Vaida, V. *J. Chem. Phys.* **2000**, *113*, 6652–6659.
- (25) Scribano, Y.; Goldman, N.; Saykally, R.; Leforestier, C. *J. Phys. Chem. A* **2006**, *110*, 5411–5419.
- (26) Atkins, P. W.; Friedman, R. S. *Molecular Quantum Mechanics*, 3rd ed.; Oxford University Press: Oxford, U.K., 1997.
- (27) Herzberg, G. *Molecular Spectra and Molecular Structure I. Spectra of Diatomic Molecules*; D. Van Nostrand Company, Inc.: Princeton, NJ, 1950.
- (28) Howard, D. L.; Jørgensen, P.; Kjaergaard, H. G. *J. Am. Chem. Soc.* **2005**, *127*, 17096–17103.
- (29) Schofield, D. P.; Kjaergaard, H. G.; Matthews, J.; Sinha, A. J. *Chem. Phys.* **2005**, *123*, 134318.
- (30) Onedim program. Olsen, J. Private Communication.
- (31) Rong, Z.; Cavagnat, D.; Lespade, L. In *Lecture Notes in Computer Science*; Sloot, P., Ed.; Springer-Verlag: Berlin, 2003; Vol. 2658, pp 350–356.
- (32) Kjaergaard, H. G.; Henry, B. R. *Mol. Phys.* **1994**, *83*, 1099–1116.
- (33) Kjaergaard, H. G.; Henry, B. R.; Wei, H.; Lefebvre, S.; Carrington, T., Jr.; Mortensen, O. S.; Sage, M. L. *J. Chem. Phys.* **1994**, *100*, 6228–6239.
- (34) Simon, S.; Duran, M.; Dannenberg, J. J. *J. Chem. Phys.* **1996**, *105*, 11024–11031.
- (35) Amos, R. D.; Bernhardsson, A.; Berning, A.; Celani, P.; Cooper, D. L.; Deegan, M. J. O.; Dobbyn, A. J.; Eckert, F.; Hampel, C.; Hetzer, G.; Knowles, P. J.; Korona, T.; Lindh, R.; Lloyd, A. W.; McNicholas, S. J.; Manby, F. R.; Meyer, W.; Mura, M. E.; Nicklass, A.; Palmieri, P.; Pitzer, R.; Rauhut, G.; Schütz, M.; Schumann, U.; Stoll, H.; Stone, A. J.; Tarroni,

R.; Thorsteinsson, T.; Werner, H.-J. *Molpro*, version 2002.1; <http://www.molpro.net>.

(36) Jung, J. O.; Gerber, R. B. *J. Chem. Phys.* **1996**, *105*, 10332–10348.

(37) Xantheas, S. S.; Dunning, T. H., Jr. *J. Chem. Phys.* **1993**, *99*, 8774–8792.

(38) Frisch, M. J.; Trucks, G. W.; Schlegel, H. B.; Scuseria, G. E.; Robb, M. A.; Cheeseman, J. R.; Montgomery, J. A., Jr.; Vreven, T.; Kudin, K. N.; Burant, J. C.; Millam, J. M.; Iyengar, S. S.; Tomasi, J.; Barone, V.; Mennucci, B.; Cossi, M.; Scalmani, G.; Rega, N.; Petersson, G. A.; Nakatsuji, H.; Hada, M.; Ehara, M.; Toyota, K.; Fukuda, R.; Hasegawa, J.; Ishida, M.; Nakajima, T.; Honda, Y.; Kitao, O.; Nakai, H.; Klene, M.; Li, X.; Knox, J. E.; Hratchian, H. P.; Cross, J. B.; Bakken, V.; Adamo, C.; Jaramillo, J.; Gomperts, R.; Stratmann, R. E.; Yazyev, O.; Austin, A. J.; Cammi, R.; Pomelli, C.; Ochterski, J. W.; Ayala, P. Y.; Morokuma, K.; Voth, G. A.; Salvador, P.; Dannenberg, J. J.; Zakrzewski, V. G.; Dapprich, S.; Daniels, A. D.; Strain, M. C.; Farkas, O.; Malick, D. K.; Rabuck, A. D.; Raghavachari, K.; Foresman, J. B.; Ortiz, J. V.; Cui, Q.; Baboul, A. G.; Clifford, S.; Cioslowski, J.; Stefanov, B. B.; Liu, G.; Liashenko, A.; Piskorz, P.; Komaromi, I.; Martin, R. L.; Fox, D. J.; Keith, T.; Al-Laham, M. A.; Peng, C. Y.; Nanayakkara, A.; Challacombe, M.; Gill, P. M. W.;

Johnson, B.; Chen, W.; Wong, M. W.; Gonzalez, C.; Pople, J. A. *Gaussian 03*, revision C.02; Gaussian, Inc.: Wallingford, CT, 2004.

(39) Kowalski, K.; Piecuch, P. *J. Chem. Phys.* **2000**, *113*, 5644–5652.

(40) Pawłowski, F.; Halkier, A.; Jørgensen, P.; Bak, K. L.; Helgaker, T.; Klopper, W. *J. Chem. Phys.* **2003**, *118*, 2539–2549.

(41) Ruden, T. A.; Helgaker, T.; Jørgensen, P.; Olsen, J. *J. Chem. Phys.* **2004**, *121*, 5874–5884.

(42) Coker, D. F.; Miller, R. E.; Watts, R. O. *J. Chem. Phys.* **1985**, *82*, 3554–3562.

(43) Slipchenko, M. N.; Kuyanov, K. E.; Sartakov, B. G.; Vilesov, A. F. *J. Chem. Phys.* **2006**, *124*, 241101.

(44) Perchard, J. P.; Mielke, Z. *Chem. Phys.* **2001**, *264*, 221–234.

(45) Rothman, L. S.; Jacquemart, D.; Barbe, A.; Benner, D. C.; Birk, M.; Brown, L. R.; Carleer, M. R.; Chackerian, C.; Chance, K.; Coudert, L. H.; Dana, V.; Devi, V. M.; Flaud, J. M.; Gamache, R. R.; Goldman, A.; Hartman, J. M.; Jucks, K. W.; Maki, A. G.; Mandin, J. Y.; Massie, S. T.; Perrian, A.; Rinsland, C. P.; Smith, M. A. H.; Tennyson, J.; Tolchenov, R. N.; Toth, R. A.; Vander Auwera, J.; Varanasi, P.; Wagner, G. *J. Quant. Spectrosc. Radiat. Transfer* **2005**, *96*, 139–204.